

Communications to the Editor

Hierarchical Structures of a Synthetic Rodlike Polyelectrolyte in Water

M. Bockstaller,^{†,‡} W. Köhler,[‡] G. Wegner,^{*,†}
D. Vlassopoulos,[§] and G. Fytas^{†,§}

Max-Planck-Institute for Polymer Research, P.O. Box 3148,
D-55128 Mainz, Germany, Physikalisches Institut
Universität Bayreuth, D-95440 Bayreuth, Germany, and
Fo.R.T.H., Institute for Electronic Structure and Laser, P.O.
Box 1527, 71110, Heraklion, Crete, Greece

Recent numerical modeling and analytical theory^{1–6} support earlier claims^{7,8} that attractive interactions between rodlike macroions of alike charge give rise to complex superstructures in aqueous solutions. The structures arise from mutual attractions of counterions which remain nonuniformly condensed near the rod surface. We introduce a simple synthetic model system that mimics some of the principal phenomena governing interactions between highly charged systems.⁹ The primary structure consists of a rigid poly(*p*-phenylene) backbone with sulfonate and dodecyl side groups (PPPS) which together render the polyelectrolyte amphiphilic. In water it forms cylindrical micelles of defined radial aggregation number $N_{\text{rad}} \sim 11^{10}$ with a negatively charged surface on account of the sulfonate groups. These micelles undergo further association to form lyotropic objects with internal nematic order on the 500 nm length scale.

PPPS is prepared by first synthesizing a parent polymer with fully protected sulfonate groups.¹¹ The parent is rigorously characterized^{11,12} (molar mass and mass distribution) before the sulfonate groups are selectively deprotected. The present sample with $R_2 = \text{C}_{12}\text{H}_{25}$ shown in Figure 1a(A) has a molar mass of 29 kg/mol, corresponding to a contour length of 53 nm and a polydispersity of $M_w/M_n = 2.1$. The persistence length

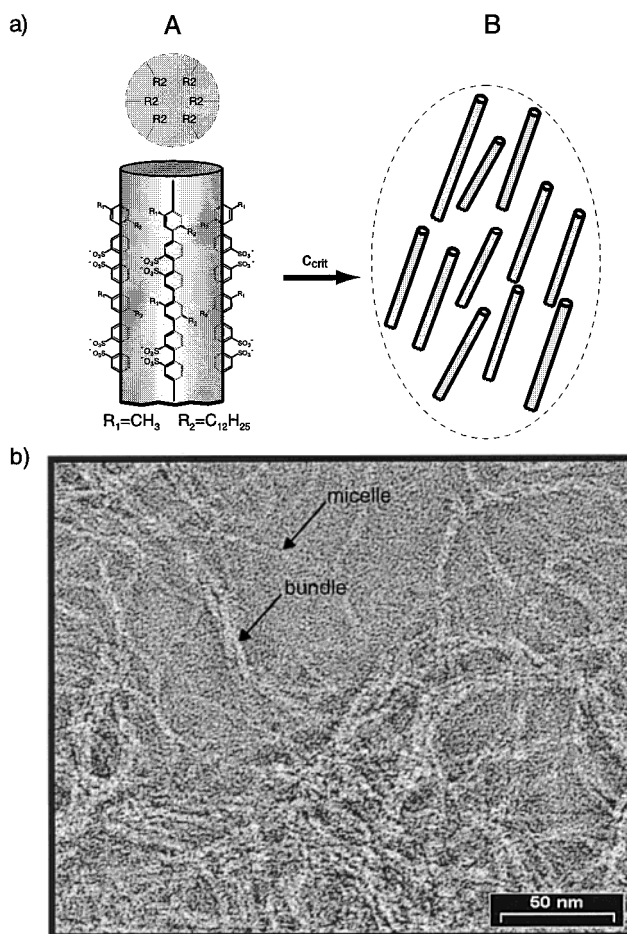


Figure 1. (a) Scheme of the self-organization of dodecyl-substituted poly(*p*-phenylene)sulfonate (PPPS) in water: (A) first aggregation step: cylindrical micelles; (B) second aggregation step: lyotropic objects ($c > 0.02$ g/L); each rod represents a cylindrical micelle as shown in (A). (b) Transmission electron micrograph of PPPS adsorbed to an amorphous carbonfilm (Philips CM 100 TEM, 100 kV).

of uncharged PPPS is about 13 nm, ensuring a wormlike

[†] Max-Planck-Institute for Polymer Research.

[‡] Physikalisches Institut Universität Bayreuth.

[§] Fo.R.T.H.

* To whom correspondence should be addressed.

conformation. Analysis of small-angle X-ray patterns of aqueous solutions of PPPS reveals the formation of cylindrical micelles with diameter $d = 3.1$ nm and a radial aggregation number $N_{\text{rad}} = 11$ independent of concentration.¹⁰ In this paper, we identify the hierarchical structures observed in the dilute regime.

An impression of the structural hierarchy observed in this system is provided by the micrograph in Figure 1b. To prepare the specimen, a carbon film was dipped into a 0.52 g/L solution and the adsorbed material was negatively stained with uranyl acetate (0.8% aqueous solution). Here, single micelles of 3.1 nm diameter coexist with bundles composed of many individual micelles. The micrograph represents a picture of the situation in solution distorted by the fact that adsorption to a surface has taken place. We attribute the bundles to objects composed of mutually aligned micelles in solution, the lyotropic objects schematically shown in Figure 1a(B). Identification of these structures in solution is best performed by static and dynamic light scattering, as both the spatial and time dependence of the distribution of scatterers can be probed.

Further, the presence of large optically anisotropic structures in solution can be best studied by dynamic depolarized light scattering.¹³ In particular, information on the rotational dynamics and internal structure of objects such as those shown in Figure 1a(B) is obtained.

In salt-free aqueous solutions single polymer molecules cannot be detected even at a concentration as low as $c = 0.001$ g/L. Instead, the polyelectrolyte exists in the form of cylindrical micelles. The relaxation function $C(q, t)$ along with the corresponding single distribution of relaxation times $G(\log(\tau/s))$ at $c = 0.008$ g/L is shown in Figure 2a. In this case, the q dependence of the Rayleigh ratio $R(q)$ obtained either from the time-averaged intensity or dynamic measurements can yield particle size and molecular weight.

The Kratky plot shown in Figure 3 suggests large structures that can be approximated by a thin rodlike shape. The length of these rods can be estimated from the translational diffusion coefficient $D = 5.2 \times 10^{-12}$ m²/s assuming cylindrical geometry with diameter $d = 3.1$ nm as obtained from SAXS measurements¹⁰ to be $L \approx 500$ nm.¹⁴ The assumption of cylindrical micelles of a given size is confirmed by TEM micrographs as in Figure 1b as well as by micrographs obtained after cryofixation.

The weight-average molar mass of these micelles can be estimated from the extrapolation of first $R(q)$ to $R(0)$ taking into account the full form factor of monodisperse rods of length $L = 500$ nm, neglecting effects of polydispersity, and second $Kc/R(0)$ to $c = 0$. The weight-average molar mass is thus calculated from the data of the inset of Figure 3 to be $M_w = 3.6 \times 10^6$ g/mol. From the molar mass of the micelles the radial aggregation number can be calculated to be $N_{\text{rad}} = 12$, in good agreement with SAXS data at higher concentrations.¹⁰ The concentration independence of the micellar size is suggested by TEM micrographs and SAXS.

With increasing concentration an abrupt change occurs in $R(q)$ and the solution dynamics. The lack of data at low magnification ($qL < 1$) renders the extrapolation to $q = 0$ ambiguous. Nevertheless, the influence of another structure above $c \approx 0.02$ g/L is evident in the plot $R(q = 8.15 \times 10^{-3} \text{ nm}^{-1})$ vs concentration (Figure 4). In fact, two distinct self-assembled aggregates contribute to $R(q)$ as demonstrated in the

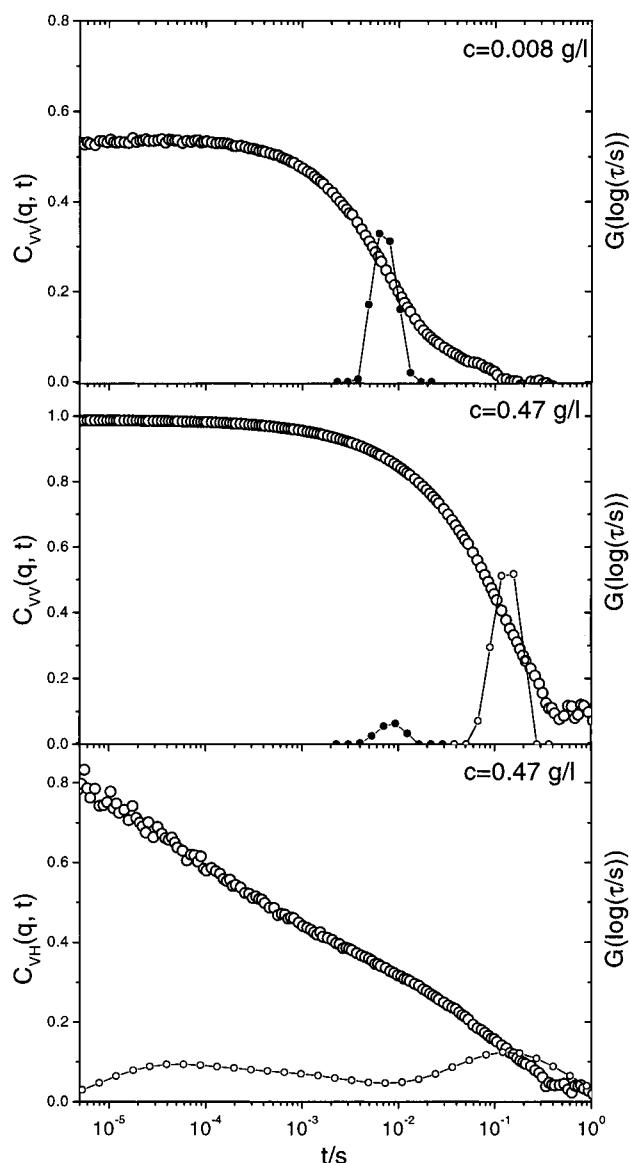


Figure 2. Relaxation function $C(q, t)$ for concentration (a, b) and orientation (c) fluctuations at $q = 8.15 \times 10^{-3} \text{ nm}^{-1}$ in salt-free aqueous solutions of PPPS at different concentrations. The filled and open symbols of $G(\log(\tau/s))$ (a, b) correspond to the cylindrical micelles A (fast) and the lyotropic objects B (slow), respectively.

bimodal concentration relaxation functions in Figure 2b. The fraction of $R(q)$ due to the fast diffusing species displays a q dependence similar to that of Figure 3 and represents the first level of ordering—the cylindrical micelles—below c_{crit} . The larger fraction of $R(q)$ is due to the slow diffusing assemblies and exhibits strong q dependence. Size and shape estimation of the large aggregates is still feasible provided that in addition to the translational diffusion the rotational diffusion is also accessible. Significant dynamic anisotropic scattering at two distinct time scales is present above the crossover concentration $c_{\text{crit}} \approx 0.02$ g/L shown in Figure 2c. The long-time dynamics relate to the rotational diffusion D_r of large scatterers. The experimental values of D and D_r at $c = 0.47$ g/L can be fitted by assuming a prolate ellipsoid with $a = 600$ nm and $b = 400$ nm for the long and short axes, respectively.¹⁵ From both static and dynamic light scattering, the emerged lyotropic objects above c_{crit} are depicted in Figure 1a(B). These objects consist of 130 micelles and are oblate spheroids. Because

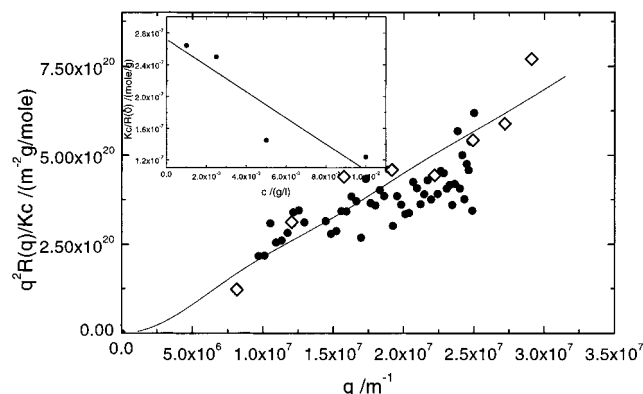


Figure 3. Kratky plot ($q^2 R(q)/c$ vs q) for PPPS in salt-free aqueous solutions at $c = 0.001$ g/L (\circ) and $c = 0.003$ g/L (\diamond) at 20 °C. $R(q)$ is the Rayleigh ratio from the static (\bullet) and dynamic (\diamond) light scattering,¹³ i.e., $\int G(\log(\tau/s)) d(\log(\tau/s))$. The inset shows the extrapolation $R(0)/Kc$ to $c = 0$ where the contrast $K = 58.4 \times 10^{-6} \text{ cm}^2 \text{ g/mol}$ for $c = 0.001, 0.0025, 0.005$, and 0.01 g/L, yielding a weight-average molar mass of $M_w = 3.6 \times 10^6$ g/mol.

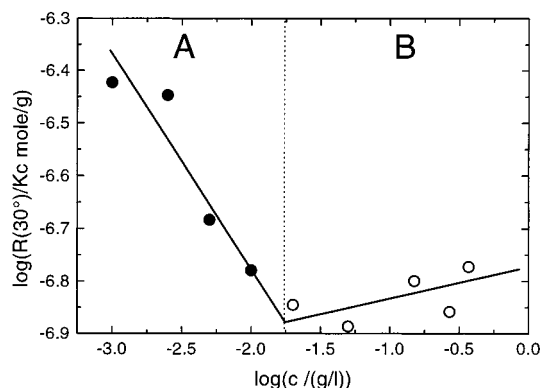


Figure 4. A double-logarithmic plot of the reciprocal reduced Rayleigh ratio $R(q = 8.15 \times 10^{-3} \text{ nm}^{-1})/c$ vs concentration of PPPS in salt-free water. A critical concentration of $c_{\text{crit}} = 0.02$ g/L separates the two regimes A and B which correspond to the structures schematically shown in Figure 1a.

of their internal anisotropic structure, their rotational diffusion could also be observed.^{12,16} Significant mobility

within these lyotropic objects is indicated by the short-time peak of $G(\log(\tau/s))$ of Figure 2c. The insensitivity of this process to concentration variations indicates an unchanged internal structure in the range 0.01–0.5 g/L.

On the basis of the present experimental evidence (Figures 1b and 2b,c), we attribute these lyotropic objects to bundle formation due to attractive interactions between the highly charged cylindrical micelles, similar to experimental evidence in the case of DNA^{17,19} and poly(L-lysine).¹⁸

Acknowledgment. This work was supported by the Deutsche Forschungsgemeinschaft grant Schu 1047 and the Max-Planck Society.

References and Notes

- (1) Holm, C.; Kremer, K. *Proceedings of Yamada Conference L-Polyelectrolytes*; Noda, I., Kokufuta, E., Eds.; Osaka, Japan, 1999; p 27f.
- (2) Jensen, N.; Mashl, R. J.; Bruinsma, R. F.; Gelbart, W. M. *Phys. Rev. Lett.* **1997**, *78*, 2477.
- (3) Stevens, M. J. *Phys. Rev. Lett.* **1999**, *82*, 101.
- (4) Oosawa, F. *Polyelectrolytes*; Marcel Dekker: New York, 1971.
- (5) Ha, B. Y.; Liu, A. J. *Phys. Rev. Lett.* **1998**, *81*, 1011.
- (6) Shlovskii, B. J. *Phys. Rev. Lett.* **1999**, *82*, 3268.
- (7) Wissenburg, P.; Odjik, T.; Cirkel, P.; Mandel, M. *Macromolecules* **1995**, *28*, 2315.
- (8) Tang, J. X.; Wong, S.; Tran, P. T.; Janmey, P. M. *Ber. Bunsen-Ges. Phys. Chem.* **1996**, *100*, 796.
- (9) Rädler, J. O.; Koltover, J.; Salditt, T.; Safinya, C. R. *Science* **1997**, *275*, 810.
- (10) Rulken, R.; Wegner, G.; Thurn-Albrecht, T. *Langmuir* **1999**, *15*, 12, 4022.
- (11) Vanhee, S.; Rosenauer, C.; Köhler, W.; Wegner, G. *Macromolecules* **1996**, *29*, 5136.
- (12) Petekidis, G.; Vlassopoulos, D.; Fytas, G.; Rulken, R.; Wegner, G. *Macromolecules* **1998**, *31*, 6129.
- (13) Berne, B.; Pecora, R. *Dynamic Light Scattering*; Wiley: New York, 1990.
- (14) Boersma, S. *J. Chem. Phys.* **1981**, *74*, 6989.
- (15) Dai, H. J.; Balsara, N. P.; Garetz, B. A.; Newstein, M. C. *Phys. Rev. Lett.* **1996**, *77*, 17.
- (16) Bockstaller, M.; Rulken, R.; Köhler, W.; Wegner, G.; Vlassopoulos, D.; Fytas, G., manuscript in preparation.
- (17) Bloomfield, V. A. *Biopolymers* **1991**, *31*, 1471.
- (18) Ise, N. *Angew. Chem.* **1986**, *98*, 323.
- (19) Seils, J.; Pecora, R. *Macromolecules* **1995**, *28*, 3, 661.

MA000190Y